6878 *Macromolecules* **1993,** *26,* 6878–6883

Asymmetric Block Copolymer Melts near the Microphase Separation Transition: A Monte Carlo Simulation

K. Binder* **and H. Fried**†

Institut für Physik, Johannes Gutenberg Universität Mainz, Staudinger Weg 7, D-55029 Mainz, Germany

Received July 15, 1993; Revised Manuscript Received September 16, 1993®

ABSTRACT: A three-dimensional lattice model of a diblock copolymer melt with composition $f = {}^3/_4$ is studied by Monte Carlo methods, extending our previous work for the symmetric case ($f = {}^1/_2$). The polymers are represented as self-avoiding walks, at a volume fraction $\phi = 0.8$ of occupied sites, and chain lengths $N = 24$, 32, and 40 are used. Different monomers at nearest-neighbor sites repel each other with an energy $k_BT\epsilon$. Due to the use of a finite lattice size $L = 32$, the microphase separation transition to the hexagonal phase can only be located rather roughly ($\epsilon_cN = 11 \pm 1$), but accurate data are obtained in the disordered phase at temperatures above the transition temperature. As in the symmetric case, we find that the Leibler theory predicts the peak of the structure factor $S(q)$ only for $\epsilon \rightarrow 0$, while the peak position q^* decreases gradually as ϵ increases by a relative amount of up to ca. 25% at the transition. Also the gyration radius of the chains increases gradually by several percent, although the gyration radii of the individual blocks even decrease slightly: the distance R_{AB} between the centers of gravity of the two blocks increases by ca. 16% up to the transition, indicating a gradual formation of asymmetric dumbell-shaped molecules. This gradual stretching of the coils sets in far above the transition, indicating a breakdown of the random phase approximation as in the symmetric case.

1. Introduction and Overview

Understanding the phase behavior of block copolymers is a challenging problem of polymer science.[1–28] Here we are concerned with simple flexible diblock copolymers, where a chain molecule of N_A monomers of type A is jointed at a junction point to a chain molecule containing N_B monomers of type B. Depending on chain length $N = N_A + N_B$, composition $f = N_A/(N_A + N_B)$, and the effective interactions between monomers of different kind (usually parametrized by the Flory–Huggins parameter χ[1–3,29]), the dense copolymer melt may exhibit various ordered superstructures ("mesophases"), such as the lamellar mesophase, where the junction points order in a layered structure, the hexagonal mesophase, where the junction points are ordered along lines which form a triangular lattice in planes perpendicular to them, and other structures.[1–5,19] While according to the simple mean field theory of Leibler[5] which is based on de Gennes'[30,31] random phase approximation (RPA), a second-order transition from the disordered phase to the lamellar phase occurs for $f = {}^1/_2$ at $\chi_cN = 10.495$, while for $f \neq {}^1/_2$ there occurs with increasing χN a sequence of first-order transitions, first to a body-centered cubic phase and then to the hexagonal phase and for still larger χN eventually to the lamellar phase, if f is not too different from $f = {}^1/_2$. This theory addresses the so-called "weak segregation regime", where it is assumed that the chains are Gaussian coils, their structure not being affected by the parameter χN. In contrast, for the limit $\chi N \rightarrow \infty$ ("strong segregation regime") the coils are stretched (gyration radius $R_g \propto N^{2/3}$ in the lamellar phase, unlike the behavior $R_g \propto N^{1/2}$ in the weak segregation regime).

While the original RPA work of Leibler[1] ignored the wave vector dependence of the third- and fourth-order vertex functions, this dependence has been included in more recent work, and as a result a chain stretching just below T_c was found.[32]

While originally it was believed that the crossover from the weak segregation limit (Gaussian chains) to the strong segregation limit (stretched chains) occurs in the ordered phase, it has been found in simulations[13–15] (and this was confirmed by some experiments[25,26]) that the onset of chain stretching occurs already well in the disordered phase. This pretransitional stretching (distinct from the stretching below T_c mentioned above[32]) implies that the RPA theory is quantitatively invalid near the transition even in the limit $N \rightarrow \infty$. For finite N also fluctuation corrections due to the Brazovskii mechanism[33] are predicted,[1,9,22] and even for $f = {}^1/_2$ the transition should be first order at a value of χN enhanced from the Leibler[5] value $\chi_cN = 10.495$ by a correction proportional to $N^{-1/3}$. Thus the theory of Fredrickson and Helfand[9] implies that there is no longer a simple scaling such that χ and N enter only via their product. Surprisingly, computer simulations carried out[14] for $f = {}^1/_2$ and very small N ($16 \leq N \leq 60$) were still compatible with the scaling of the data in terms of the Leibler[5] variable χN, although in other respects strong deviations from RPA were found: coil stretching occurs for temperatures T distinctly above T_c; the plot of the inverse structure function at its maximum, $S^{-1}(q^*)$, versus χN (or ϵN, respectively) is distinctly curved and not linear as the theory[5] predicts; $x^* \equiv q^*R_g$ is not constant in the disordered phase ($x^* = 1.95$ for $f = {}^1/_2$[5]) but rather decreases distinctly ($x^* \approx 1.5$ at the transition[13,14]).

At this point a full theoretical understanding of the ordering behavior of block copolymers has not been reached. Monte Carlo simulations should yield very useful insight into this question, avoiding some of the problems that may hamper experiments: any asymmetry in the size and shape of the monomers (which may in real systems be a very important parameter!) can be strictly avoided; the model is constructed such that there is no glass transition, and thus the full regime of all temperatures, $0 \leq \epsilon < \infty$, is at one's disposal; it is straightforward to obtain very detailed information (e.g., the collective structure factor $S(q)$ describing the fluctuations in volume fraction can be obtained simultaneously with the geometrical characteristics of single chains, such as gyration

---

† Present address: Apartment No. 1, 743 Packard, Ann Arbor, MI 48104.

® Abstract published in *Advance ACS Abstracts,* November 1, 1993.

0024-9297/93/2226-6878$04.00/0

radii of individual blocks R_g^A and R_g^B or the distance R_{AB} between their centers of gravity, etc.). Thus the interplay between chain configurational statistics and thermodynamics can be stringently tested.

Thus in the present work we extend our previous Monte Carlo studies of symmetric diblock copolymer melts[13-15] to the asymmetric case, presenting here results for $f = {}^3/_4$. Since the chain lengths accessible to our study are relatively short ($24 \leq N \leq 40$) and since it would not make sense to simulate blocks which contain less than 6 monomers of one kind only, we have not attempted to study more asymmetric cases yet. For $f = {}^3/_4$, however, both the Leibler theory[5] and the theory of Fredrickson and Helfand[9] predict an extended range of stability of the hexagonal phase, and inspection of snapshot pictures of configurations obtained from our simulation at low temperature (large ϵ) shows that this structure is indeed the ordering obtained from our model. We are hence interested to check whether the strong deviations from the RPA found for the symmetric case carry over to the present situation, too.

In section 2, we briefly summarize the main technical aspects of our simulations and specify the quantities that are calculated. Section 3 presents our numerical results and gives a comparison with the symmetric case, while section 4 summarizes our conclusions.

2. Model and Simulation Technique

We consider simple cubic $L \times L \times L$ lattices with periodic boundary conditions, representing the polymer chains as self-avoiding and mutually avoiding walks on the lattice as in refs 13–15. Each site is taken by an A-monomer, a B-monomer, or a vacancy, choosing a volume fraction $\phi_V = 0.2$ of vacancies throughout. In our model, the physical consequences of vacancies are twofold: (i) They are necessary for rapid equilibration, ensuring a high chain mobility when the "slithering-snake"[13-15,34-37] algorithm is used. (ii) They ensure that the polymer melt has a small but nonzero compressibility and are hence necessary for corresponding physical effects such as a reduced polymer density in the A–B interfaces in the strongly segregated case,[38] etc. Therefore there is no real advantage to use models which have $\phi_V = 0$[18] and are moreover hampered by the slowness of the algorithm, which then is necessarily much more complicated to implement and also gives rise to slowly decaying dynamic correlations between configurations which are less well understood than for the standard algorithms.[35] Of course, it is a matter of concern whether a fraction of vacancies $\phi_V = 0.2$ is perhaps too large and then might give rise to unphysical effects: however, both for the case of polymer blends[39] and for the case of symmetrical block copolymers[18,40] the vacancy content ϕ_V was varied over a wide range and it was found that the precise value of ϕ_V affects only quantitative details such as location of the transition ϵ_c, the scale of the collective structure factor $S(q)$, etc., but all qualitative features of the results are completely independent of ϕ_V as long as $\phi_V \lesssim 0.5$.

The chains experience also repulsive interaction $\epsilon_{AB} > 0$ which acts between all nearest-neighbor pairs of unlike monomers in the lattice. This energy parameter acts in the standard Metropolis transition probability[35,36] applied for all Monte Carlo moves. No energy parameters enter between AA pairs or BB pairs or involve the vacancies, respectively. We then define $\epsilon \equiv \epsilon_{AB}/k_BT$.

Apart from the "slithering-snake" motions, where the A–B junction point must move by one unit along the chain,[14] we also apply head-to-tail interchanges of the chain, where the A–B junction point has to move by $N_A - N_B$ units along the chain when the move is accepted. This move is the generalization of the A–B interchange applied previously in the symmetric case[14] (where the A–B junction does not move) to asymmetric block copolymers. We find this move rather effective in destroying dynamic correlations between fluctuations of the local concentrations.

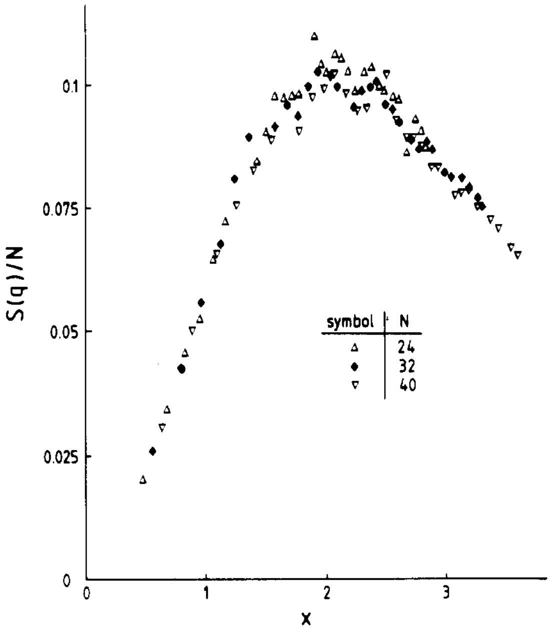

Figure 1. Plot of normalized spherically averaged collective structure factor $S(q)/N$ vs the variable $x = qR_g$, R_g being the gyration radius of the chains, for the athermal diblock copolymer melt with $f = {}^3/_4$. Three choices of N are shown as indicated in the figure.

In our previous work on symmetric diblocks[14] the lattice linear dimensions were varied from $L = 16$ to $L = 32$ for $N = 16$, but within the rather limited statistical accuracy no clear evidence for finite size effects was found throughout the disordered phase of the block copolymer melt. For the sake of an efficient use of computer time, we work here with a single linear dimension $L = 32$ for all N. A consequence of the finiteness of L and the periodic boundary condition is that the collective structure factor $S(\vec{q})$ is defined for discrete values $\vec{q}_{\nu_x,\nu_y,\nu_z}$ only,

$$\vec{q}_{\nu_x,\nu_y,\nu_z} = \frac{2\pi}{L}(\nu_x,\nu_y,\nu_z), \qquad \nu_x,\nu_y,\nu_z \text{ integer} \tag{1}$$

While this discreteness of reciprocal space is no serious drawback in the disordered phase (see Figure 1), deep in the ordered phase a wavelength λ^* as large as $\lambda^* \approx 16$ lattice spacings is observed for $N = 40$, and this means that the ordered structure is strongly affected by the finite size of the system: the box can accommodate just a few B-rich cylinders in the A-rich background only; and the commensurability of the hexagonal mesophase with the cubic box (and the periodic boundary condition) in general will be a serious disturbance of this structure. This problem can be avoided only if substantially larger lattice sizes were used, and hence no study of the ordered phase was attempted.

Associating a pseudospin variable $\sigma(\vec{r}) = -1,0,1$ with a lattice site $\vec{r}$ taken by an A monomer, a vacancy V, or a B monomer, respectively, we define the structure factor $S(\vec{q})$ as the Fourier transform of the "pseudospin" correlation function in the system

$$S(\vec{q}) = L^{-3}\sum_{i,j}\exp\{i\vec{q}\cdot(\vec{r}_i - \vec{r}_j)\}[\langle\sigma(\vec{r}_i)\,\sigma(\vec{r}_j)\rangle_T - \langle\sigma(\vec{r}_i)\rangle_T\langle\sigma(\vec{r}_j)\rangle_T] \quad (2)$$

Remember that in the incompressible limit (considered by the standard RPA[5]) the concentration correlation function of species A (or B, respectively) is related to this pseudospin correlation in eq 2 as

$$\langle\phi_A(\vec{r}_i)\,\phi_A(\vec{r}_j)\rangle - \langle\phi_A(\vec{r}_i)\rangle\langle\phi_A(\vec{r}_j)\rangle \equiv [\langle\sigma(\vec{r}_i)\,\sigma(\vec{r}_j)\rangle_T - \langle\sigma(\vec{r}_i)\rangle_T\langle\sigma(\vec{r}_j)\rangle_T]/4$$

using $\phi_A(\vec{r}) = [1 - \sigma(\vec{r})]/2$, and $\phi_B(\vec{r}) = [1 + \sigma(\vec{r})]/2$.

To improve the statistics, we carry out a spherical average in q-space. This yields the quantity $S(q)$ shown in Figure 1. Although our chains are very short, it is seen that the normalized quantity $S(q)/N$ yields an essentially N-independent result, characteristic for the limiting behavior $N \to \infty$. The RPA predicts[5]

$$NS^{-1} = -2\chi N + g_D(1,x^2)/\Big\{g_D(f,x^2)\,g_D(1-f,x^2) - \frac{1}{4}[g_D(1,x^2) - g_D(f,x^2) - g_D(1-f,x^2)]^2\Big\} \quad (3)$$

where $x = qR_{gyr} = qa(N/6)^{1/2}$, a being an effective segment size, and $g_D(f,x^2)$ is the Debye function

$$g_D(f,x^2) = 2\{f + [\exp(-fx^2) - 1]/x^2\}/x^2 \quad (4)$$

From eqs 3 and 4 it is obvious that the maximum of $S(\vec{q})$ occurs at a value of x which is independent of χN and depends on f only. For $f = {}^3/_4$ one finds that this maximum occurs for $x^* \equiv q^*R_{gyr} \cong 2.053$. It is seen from Figure 1 that the numerical data for the athermal model are compatible with this RPA prediction, as expected. Already in our work on symmetrical block copolymers[14] it was shown that the simulation data can be fitted quantitatively to the Leibler RPA throughout the disordered phase if one treats χ and R_{gyr} as adjustable parameters, rather than assuming $\chi \propto \epsilon$ and taking the gyration radius as observed in the simulation.

Being interested in a test of the RPA for the present asymmetric case as well, we sample the following geometric characteristics of the chains: the gyration radius R_g as well as the gyration radii R_g^A and R_g^B of the A- and B-blocks,

$$R_g(\epsilon,N) \equiv \langle\sum_{n=1}^{N}(\vec{R}_n - \vec{R}_{CM})^2\rangle_T^{1/2} \quad (5)$$

$$R_g^A(\epsilon,N) \equiv \langle\sum_{n=1}^{N_A}(\vec{R}_n^A - \vec{R}_{CM}^A)^2\rangle_T^{1/2} \quad (6)$$

and

$$R_g^B(\epsilon,N) \equiv \langle\sum_{n=1}^{N_B}(\vec{R}_n^B - \vec{R}_{CM}^B)^2\rangle_T^{1/2} \quad (7)$$

where $\vec{R}_{CM}$ is the center of mass position of the whole chain, $\vec{R}_{CM}^A$ the center of mass position of the A-block, and $\vec{R}_{CM}^B$ the center of mass position of the B-block. While in eq 5 the sum is extended over all monomers of a chain, in eq 6 one sums only over the monomers of type A and in eq 7 over the monomers of type B. The statistical average $\langle ... \rangle_T$ includes an average over all chains in a system configuration and over all equilibrated configurations used for the thermal averaging at the considered temperature. The center of mass vectors are defined as

$$\vec{R}_{CM} = N^{-1}\sum_{n=1}^{N}\vec{R}_n, \quad \vec{R}_{CM}^A = N_A^{-1}\sum_{n=1}^{N_A}\vec{R}_n^A, \quad \vec{R}_{CM}^B = N_B^{-1}\sum_{n=1}^{N_B}\vec{R}_n^B \quad (8)$$

$\vec{R}_n = (\vec{R}_n^A$ or $\vec{R}_n^B)$ being the nth monomer in a chain (or block, respectively). We also obtain the average mean square distance between the centers of gravity of the blocks,

$$R_{AB}(\epsilon,N) \equiv \langle(\vec{R}_{CM}^A - \vec{R}_{CM}^B)^2\rangle_T^{1/2} \quad (9)$$

which is a good indicator for the stretching of the chains.

Finally, we obtain the principal radii $R_i(\epsilon,N)$ of the copolymer ($i = 1,2,3$) which are defined in terms of the principal moments I_i of the copolymer moment of inertia tensor as

$$R_i = (R_g^2 - I_i/N)^{1/2} \quad (10)$$

For a Gaussian chain one has[41]

$$(R_1/R_g)^2 \cong 0.76, \quad (R_2/R_g)^2 \cong 0.176, \quad (R_3/R_g)^2 \cong 0.065 \quad (11)$$

while we find for our chains (N = 24, 32, and 40) for $\epsilon = 0$

$$(R_1/R_g)^2 \cong 0.767, \quad (R_2/R_g)^2 \cong 0.171, \quad (R_3/R_g)^2 \cong 0.062 \quad (12)$$

These numbers are quite close to the Gaussian results and show that despite the presence of the vacancies our chains behave as Gaussian coils, as it should be in a dense melt.

As for the symmetric case, we consider the correlation time for the direction of $\vec{q}$ for which $S(\vec{q})$ has the most intensity and locate the microphase separation transition ϵ_c from the condition that this correlation time grows to a very large value (i.e., several thousand Monte Carlo steps [MCS] per monomer). All data are based on runs of 10^4 MCS, averages being taken at intervals of 10^2 MCS. As in the symmetric case, a quasistatic cooling procedure is used (the last lattice configuration of the simulation at ϵ is used as the first lattice configuration at $\epsilon + \delta\epsilon$, the first 5000 MCS at the new temperature being omitted for thermalization before averaging is started. Since we have about 10–18 values of ϵ from the athermal limit ($\epsilon = 0$) to the microphase separation transition ($\epsilon = \epsilon_c$), our increment $\delta\epsilon$ in inverse temperature is reasonably small. An important fact is also that the acceptance rate A of the slithering-snake moves is reasonably large throughout (see Figure 2), even at temperatures below the microphase separation transition. As expected, the acceptance rate does not depend on N and follows a simple Arrhenius law, $A \approx 0.73\exp(-1.2\epsilon)$; i.e., the activation energy is of order unity.

3. Results for the Collective Structure Factor and for the Chain Radii

Figure 3 presents the collective structure function $S(x,\epsilon)$ for $N = 40$. The general behavior is very similar to the findings for $f = {}^1/_2$; i.e., on the scale of $x = qR_g(\epsilon,N)$ the peak position is not constant but shifts from its value predicted by the RPA ($x^* \approx 2.053$) to smaller values as ϵ increases. Data for other choices of ϵ and the two smaller values of N look very similar, as expected from Figure 1. Figure 4 shows a plot of the inverse $NS^{-1}(x^*)$ of the maximum scattering intensity plotted vs ϵN. According

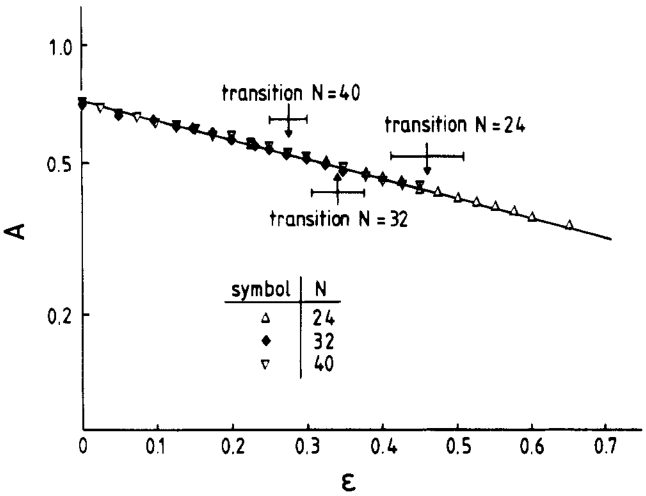

Figure 2. Semilogarithmic plot of the acceptance rate A of "slithering-snake" moves versus ϵ. Three values of N are shown as indicated. Arrows show the estimated transition to the hexagonal ordered phase.

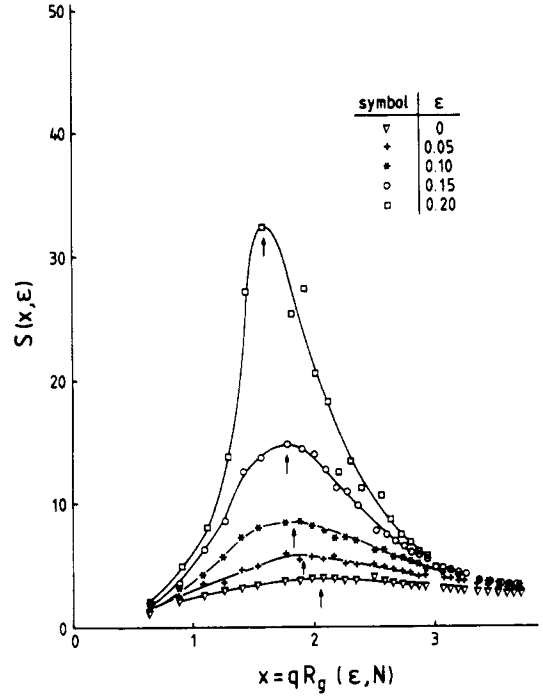

Figure 3. Collective structure factor $S(x,\epsilon)$ plotted vs $x = qR_g(\epsilon,N)$ for $N = 40$, $f = {}^3/_4$, and several values of ϵ as indicated. Arrows show estimates for $x^*(\epsilon,N)$. Note that due to the finite size of L (and periodic boundary conditions), $S(x,\epsilon)$ is defined for discrete values of q only, given by the symbols; smooth curves are guides to the eye only.

to the Leibler RPA,[5] this plot should be simple straight line which hits the abscissa at the spinodal. Just as for the symmetric case,[13,14] we find a very strong curvature, which is also seen in corresponding experiments.[24-26] At the first-order transition, ideally there should be a jump-like singular decrease of $S^{-1}(x^*)$ due to the onset of long-range order, but this is smeared out in our small lattices and hence is not seen. We also note that the theory of Fredrickson and Helfand[9] implies that $NS^{-1}(x^*)$ is a nonlinear function of ϵ, but there should be systematic corrections (of order $N^{-1/3}$) to the leading order terms and hence there must be systematic deviations from the scaling with ϵN. However, since the range from $N = 24$ to $N = 40$ only means a range of $N^{-1/3}$ from 0.347 to 0.292, it hence is quite possible that such corrections are not resolved in Figure 4, due to the appreciable statistical scatter of these data.

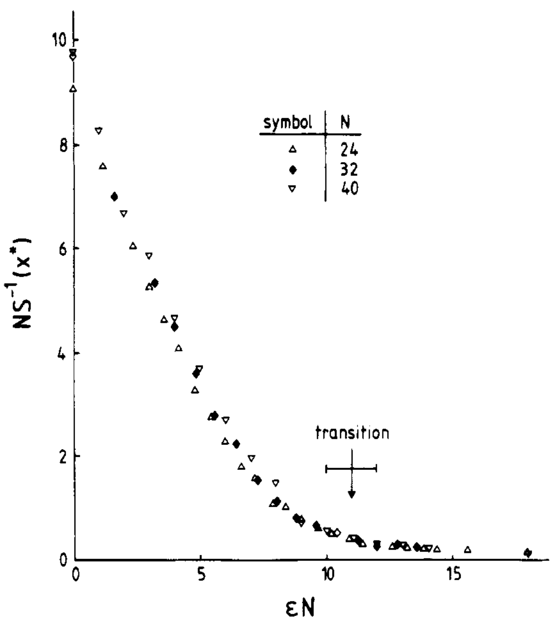

Figure 4. Plot of normalized inverse intensity $NS^{-1}(x^*)$ at the wave vector $q^* = x^*/R_g$, where maximum scattering occurs, vs ϵN for $f = {}^3/_4$ and three values of N as indicated. Arrow shows the approximate location of the transition to the hexagonal phase, which is located from an analysis of the relaxation time.

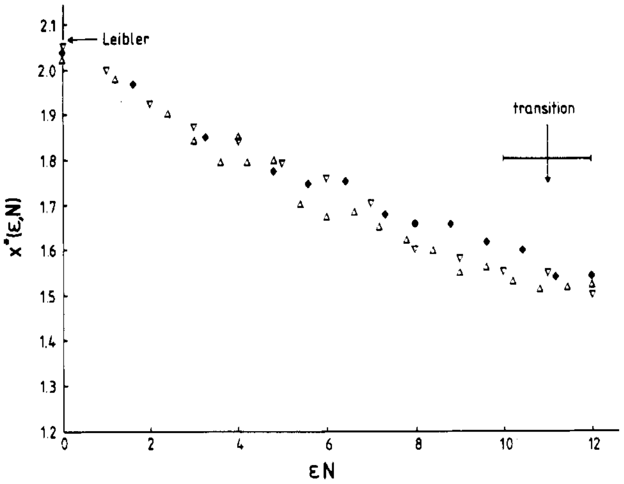

Figure 5. Peak position $x^*(\epsilon,N) = q^*R_g(\epsilon,N)$ where $S(q,\epsilon)$ has its maximum plotted vs ϵN for $f = {}^3/_4$ and $N = 24$ (upward-pointing triangles), $N = 32$ (diamonds), and $N = 40$ (downward-pointing triangles).

Figure 5 shows the variation of the peak position $x^*(\epsilon,N)$ with ϵN for $f = {}^3/_4$. It is interesting to compare these data with corresponding results for the symmetrical case. Apart from the fact that for $f = {}^1/_2$ the transition occurs earlier {for $\epsilon_c N \approx 8.3 \pm 0.7$ $(f = {}^1/_2)$[14] instead $\epsilon_c N = 11 \pm 1$ $(f = {}^3/_4)$}, the behavior is qualitatively similar: x^* decreases from 2.053 to about 1.53 for $f = {}^3/_4$ (i.e., a relative decrease of about 25%), and x^* decreases from 1.95 to about 1.45 for $f = {}^1/_2$ (again a relative decrease of about 25%). The increase of ϵ_c when f deviates from $f = {}^1/_2$ is already expected from the Leibler RPA:[5] $\chi_c N(f={}^1/_2) = 10.495$ while $\chi_c N(f={}^3/_4) = 18.2$ at the spinodal, $\chi_c N(f={}^3/_4) = 17.6$ at the first-order transition. The theory of Fredrickson and Helfand[9] predicts a somewhat smaller increase of ϵ_c with $f = {}^1/_2$, and thus is somewhat closer to the observed behavior than Leibler's theory. However, since this theory[9] is believed to be qualitatively valid only for $N \geq 10^4$, we do not attempt to compare it with our simulations on a quantitative level.

Very interesting is the behavior of the gyration radii (Figure 6): while the total radius $R_g(\epsilon,N)$ starts to increase

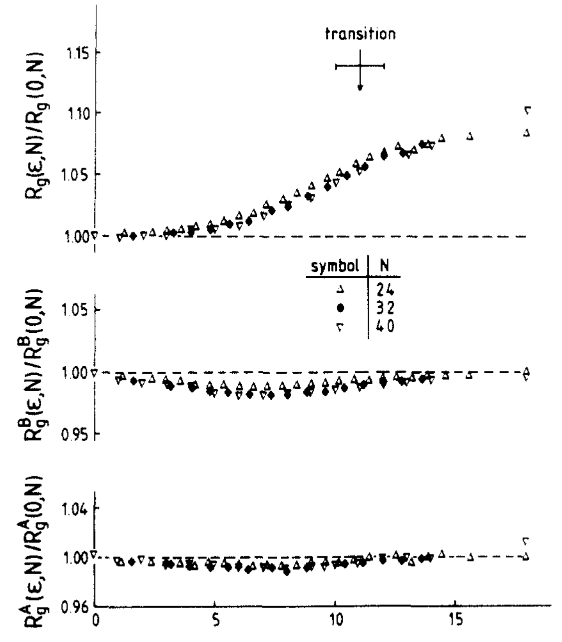

Figure 6. Normalized gyration radius $R_g(\epsilon,N)/R_g(0,N)$ of the total chain (upper part), of the short block $\{R_g^B(\epsilon,N)/R_g^B(0,N)\}$ (middle part), and of the long block $\{R_g^A(\epsilon,N)/R_g^A(0,N)\}$ (bottom part) for $f = 3/4$ plotted vs ϵN. Three choices of N are included as indicated in the figure. Arrow shows the estimated location of the microphase separation transition.

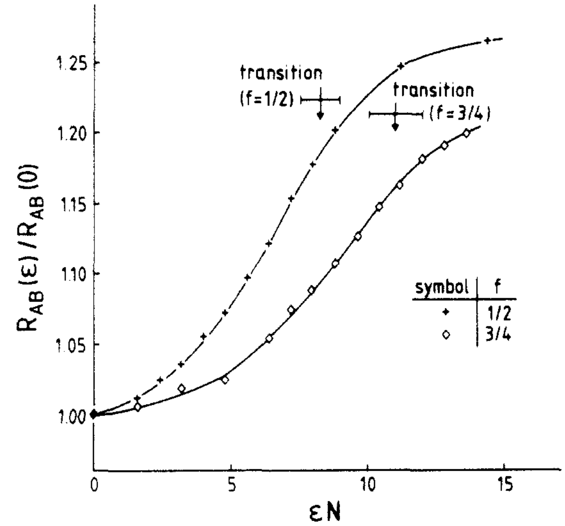

Figure 7. Normalized distance between the centers of gravity of the two blocks, $R_{AB}(\epsilon)/R_{AB}(0)$, plotted for $N = 32$ vs ϵN, comparing data for $f = 1/2$ and $f = 3/4$.

relative to its athermal value $R_g(0,N)$ already for $\epsilon N \gtrsim 4$, i.e., at temperatures that are more than a factor 2 higher than the transition temperature, the radii $R_g^A(\epsilon,N)$ and $R_g^B(\epsilon,N)$ rather show a slight decrease. The individual blocks thus behave as chains do in binary AB blends, which also show some decrease of the radii with increasing N,[39] and there it also is observed that the minority chains contract stronger than the majority chains do. The overall increase of $R_g(\epsilon,N)$, which thus is opposite to the tendency of the individual blocks, is due to an increasing of the ditance between the centers of gravity of the two blocks (Figure 7). This tendency is qualitatively the same as for $f = 1/2$, but quantitatively it is somewhat less pronounced. While for $f = 1/2$ the shape of a block copolymer near the microphase separation transition hence is that of a symmetric dumbell, where unfavorable AB contacts are reduced by stretching the coil, we now have an unsymmetric dumbell. The larger ϵ is, the more elastic energy due to the stretching can be balanced by the energy gain due to avoiding the unfavorable contacts, of course. This coil to dumbell transition is a gradual change in the chain conformation, and no sharp phase transition is involved. Unlike the stretching of polymer chains in polymer brushes, where more or less the whole chain is stretched uniformly,[42] the chain deformation here is strongly nonuniform, since the two blocks themselves become somewhat contracted and it is their relative distance that increases. We also emphasize that all behavior that is seen in Figures 6 and 7 is not contained in the Leibler RPA,[5] and since we expect that these effects remain present even in the limit $N \rightarrow \infty$, the latter theory does not acount for important aspects of the microphase separation in block copolymers. The present work shows that this breakdown of the simple form of the RPA as used in ref 5 is not restricted to $f = 1/2$ but presumably occurs for all values of f.

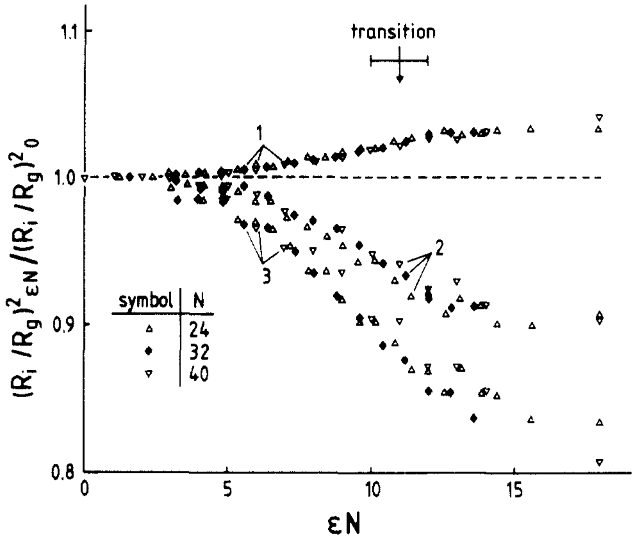

Figure 8. Plot of the normalized principal radii $(R_i/R_g)_{\epsilon N}^2/(R_i/R_g)_0^2$ vs ϵN for $f = 3/4$ and three choices of N as indicated.

The same conclusion about the stretching of the chains can be obtained from a study of the principal radii R_i (Figure 8). The decrease of R_i for $i = 2,3$ is consistent with the contraction of the individual blocks of the copolymer chains. An interesting feature is that the relative decrease for $(R_2/R_g)_{\epsilon N}^2/(R_2/R_g)_0^2$ and $(R_3/R_g)_{\epsilon N}^2/(R_3/R_g)_0^2$ is the same for $f = 1/2$[15] but different for $f = 3/4$: this distinction probably reflects the reduction of symmetry of the asymmetric dumbell in comparison to the symmetric one.

4. Concluding Remarks

In the present Monte Carlo simulation of diblock copolymer melts with asymmetric composition ($f = 3/4$) the interplay between single-chain properties and the development of a collective length scale describing the concentration inhomogeneities has been elucidated. While qualitatively the collective structure factor (Figures 1 and 3) always resembles the prediction of the Leiber RPA,[5] the latter is quantitatively useful in the limit of very weak interactions only. At temperatures where in a binary blend with chain lengths comparable to those of the individual blocks macroscopic phase separation would set in, already strong local segregation starts to develop, the A-blocks and B-blocks start to contract slightly, and at the same time the distance between their centers of gravity starts to increase distinctly. Qualitatively, this type of behavior is understandable with treatments based on the Edwards Hamiltonian,[12,18] and it is hoped that our results will stimulate the development of a theory that describes these effects quantitatively. By this chain stretching the resulting symmetric dumbells (for $f = {}^1/_2$) form clusters where they develop orientational short-range order like in a nematic liquid crystal, and in this way a characteristic wavelength $\lambda^* = 2\pi/q^*$ of lamellar short-range order may develop that differs from R_{AB} itself.[13,15] For the asymmetric case ($f = {}^3/_4$) asymmetrical dumbells develop but again the numerical data imply that there is no straightforward relation between single-chain length scales and the collective scale: at the transition, λ^* has increased by about 25% (Figure 5) but R_{AB} has increased only by about 16% (Figure 7). It is hoped that our results will stimulate further theoretical work including these changes in chain conformation that occur already in the disordered phase into the description of the order–disorder transition. Also experiments where individual blocks and individual whole chains are labeled by deuteration and chain linear dimensions are measured by neutron scattering would be very desirable. Since the predicted effects are not large and good accuracy is required, these experiments unfortunately are not straightforward. We believe, however, that the behavior found in this work has also consequences for the behavior of block copolymers adsorbed to interfaces or surfaces, ternary mixtures involving block copolymers, etc. It would also be very interesting to extend the present simulation studies into the strongly segregated low-temperature phase.

Acknowledgment. H.F. received support from the Max Planck Institut für Polymerforschung, Mainz. We are grateful to A. Weyersberg for a preprint of ref 18.

References and Notes

(1) For reviews of theoretical work, see: Bates, S. F.; Fredrickson, G. H. *Annu. Rev. Phys. Chem.* **1990**, *41*, 525, and refs 2 and 3; for recent experiments, see: refs 24–28.

(2) Brown, R. A.; Masters, A. J.; Price, C.; Yuan, X. F. In *Comprehensive Polymer Science*; Allen, G., Ed.; Pergamon Press: Oxford, 1989; p 155.

(3) Binder, K. *Adv. Polym. Sci.*, in press.

(4) Helfand, E.; Wassermann, Z. R. *Macromolecules* **1976**, *9*, 876.

(5) Leibler, L. *Macromolecules* **1980**, *13*, 1602.

(6) Hong, K. M.; Noolandi, J. *Macromolecules* **1981**, *14*, 727; **1983**, *17*, 1443. Noolandi, J.; Hong, K. M. *Macromolecules* **1982**, *15*, 482.

(7) Semenov, A. N. *Sov. Phys.—JETP* **1985**, *61*, 733.

(8) Ohta, T.; Kawasaki, K. *Macromolecules* **1986**, *19*, 2621. Kawasaki, K.; Ohta, T.; Kohrogu, M. *Macromolecules* **1988**, *21*, 2972.

(9) Fredrickson, G. H.; Helfand, E. *J. Chem. Phys.* **1987**, *87*, 697.

(10) Fredrickson, G. H.; Binder, K. *J. Chem. Phys.* **1989**, *91*, 7265.

(11) Burger, C.; Ruland, W.; Semenov, A. N. *Macromolecules* **1990**, *23*, 3339.

(12) Borsali, R.; Vilgis, T. A. *J. Chem. Phys.* **1990**, *92*, 3610. Vilgis, T. A.; Benmouna, M.; Benoit, H. *Macromolecules* **1991**, *24*, 4482.

(13) Minchau, B.; Dünweg, B.; Binder, K. *Polym. Commun.* **1990**, *31*, 8349.

(14) Fried, H.; Binder, K. *J. Chem. Phys.* **1991**, *94*, 8349.

(15) Fried, H.; Binder, K. *Europhys. Lett.* **1991**, *16*, 237.

(16) Kikuchi, M.; Binder, K. *Europhys. Lett.* **1993**, *21*, 427.

(17) Chakrabarti, A.; Toral, R.; Gunton, J. D. *Phys. Rev. Lett.* **1989**, *63*, 2661; *Phys. Rev. A* **1991**, *A44*, 6563.

(18) Weyersberg, A.; Vilgis, T. A. *Phys. Rev. E*, in press.

(19) Olvera de la Cruz, M. *Phys. Rev. Lett.* **1991**, *67*, 85. Olvera de la Cruz, M.; Mayes, A. M.; Swift, B. W. *Macromolecules* **1992**, *25*, 944.

(20) Melenkovitz, J.; Muthukumar, M. *Macromolecules* **1991**, *24*, 4199.

(21) Holyst, R.; Schick, M. *J. Chem. Phys.* **1992**, *96*, 7728.

(22) Barrat, J. L.; Fredrickson, G. H. *J. Chem. Phys.* **1991**, *95*, 1281.

(23) Tang, H.; Freed, K. F. *J. Chem. Phys.* **1992**, *96*, 8621.

(24) Bates, F. S.; Rosedale, J. H.; Fredrickson, G. H. *J. Chem. Phys.* **1990**, *92*, 6255.

(25) Almdal, K.; Rosedale, J. H.; Bates, F. S.; Wignall, G. D. *Phys. Rev. Lett.* **1990**, *65*, 1112.

(26) Stühn, B.; Mutter, R.; Albrecht, T. *Europhys. Lett.* **1992**, *18*, 427.

(27) Stühn, B.; Stickel, F. *Macromolecules* **1992**, *25*, 5306.

(28) Alig, I.; Kremer, F.; Fytas, G.; Roovers, J. *Macromolecules* **1992**, *25*, 5277.

(29) Flory, P. J. *Principles of Polymer Chemistry*; Cornell University Press: Ithaca, NY, 1953.

(30) De Gennes P.-G. *J. Phys. (Paris)* **1970**, *31*, 235.

(31) De Gennes, P.-G. *Scaling Concepts in Polymer Physics*; Cornell University Press: Ithaca, NY, 1979.

(32) Tang, H.; Freed, K. F. *J. Chem. Phys.* **1991**, *95*, 3012. Shull, K. R. *Macromolecules* **1992**, *25*, 2122. McMullen, W. E. *Macromolecules* **1993**, *26*, 1027.

(33) Brazovskii, S. A. *Sov. Phys.—JETP* **1975**, *41*, 85.

(34) For a comparative discussion of various algorithms for lattice models of polymers, the reader may consult refs 35 and 36; the slithering-snake algorithm for homopolymers was first used in ref 37.

(35) Kremer, K.; Binder, K. *Comput. Phys. Rep.* **1988**, *7*, 259.

(36) Baumgärtner, A. In *Applications of the Monte Carlo Method in Statistical Physics*; Binder, K., Ed.; Springer: Berlin, 1984; Chapter 5.

(37) Kron, A. K. *Polym. Sci. USSR (Engl. Transl.)* **1965**, *7*, 1361. Wall, F. T.; Mandel, F. *J. Chem. Phys.* **1975**, *63*, 4592.

(38) Kikuchi, M.; Binder, K., preprint.

(39) Sariban, A.; Binder, K. *Macromolecules* **1988**, *21*, 711.

(40) Fried, H.; Binder, K., unpublished.

(41) Kranbuehl, D.; Verdier, P. *J. Chem. Phys.* **1977**, *67*, 361.

(42) Halperin, A.; Tirrell, M.; Lodge, T. P. *Adv. Polym. Sci.* **1991**, *100*, 31.